JVI Journals.ASM.org

# Virus-Specific Memory CD8 T Cells Provide Substantial Protection from Lethal Severe Acute Respiratory Syndrome Coronavirus Infection

**Rudragouda Channappanavar,[a] Craig Fett,[a] Jincun Zhao,[a] David K. Meyerholz,[b] Stanley Perlman[a]**

Departments of Microbiology,[a] and Pathology,[b] University of Iowa, Iowa City, Iowa, USA

**ABSTRACT**

**Severe acute respiratory syndrome coronavirus (SARS-CoV) caused an acute human respiratory illness with high morbidity and mortality in 2002-2003. Several studies have demonstrated the role of neutralizing antibodies induced by the spike (S) glycoprotein in protecting susceptible hosts from lethal infection. However, the anti-SARS-CoV antibody response is short-lived in patients who have recovered from SARS, making it critical to develop additional vaccine strategies. SARS-CoV-specific memory CD8 T cells persisted for up to 6 years after SARS-CoV infection, a time at which memory B cells and antivirus antibodies were undetectable in individuals who had recovered from SARS. In this study, we assessed the ability of virus-specific memory CD8 T cells to mediate protection against infection in the absence of SARS-CoV-specific memory CD4 T or B cells. We demonstrate that memory CD8 T cells specific for a single immunodominant epitope (S436 or S525) substantially protected 8- to 10-month-old mice from lethal SARS-CoV infection. Intravenous immunization with peptide-loaded dendritic cells (DCs) followed by intranasal boosting with recombinant vaccinia virus (rVV) encoding S436 or S525 resulted in accumulation of virus-specific memory CD8 T cells in bronchoalveolar lavage fluid (BAL), lungs, and spleen. Upon challenge with a lethal dose of SARS-CoV, virus-specific memory CD8 T cells efficiently produced multiple effector cytokines (gamma interferon [IFN-γ], tumor necrosis factor alpha [TNF-α], and interleukin 2 [IL-2]) and cytolytic molecules (granzyme B) and reduced lung viral loads. Overall, our results show that SARS-CoV-specific memory CD8 T cells protect susceptible hosts from lethal SARS-CoV infection, but they also suggest that SARS-CoV-specific CD4 T cell and antibody responses are necessary for complete protection.**

**IMPORTANCE**

**Virus-specific CD8 T cells are required for pathogen clearance following primary SARS-CoV infection. However, the role of SARS-CoV-specific memory CD8 T cells in mediating protection after SARS-CoV challenge has not been previously investigated. In this study, using a prime-boost immunization approach, we showed that virus-specific CD8 T cells protect susceptible 8- to 10-month-old mice from lethal SARS-CoV challenge. Thus, future vaccines against emerging coronaviruses should emphasize the generation of a memory CD8 T cell response for optimal protection.**

Coronaviruses belong to a group of pathogens that periodically emerge from zoonotic sources to infect human populations, often resulting in high rates of morbidity and mortality (1–3). Severe acute respiratory syndrome coronavirus (SARS-CoV) and Middle East respiratory syndrome coronavirus (MERS-CoV) are two notable examples of novel coronaviruses that emerged during the last decade (1, 2, 4). Infection with these coronaviruses can result in the acute respiratory distress syndrome (ARDS), which has a high rate of morbidity and mortality (3, 5). SARS-CoV infected humans during 2002-2003 and caused a global epidemic, spreading rapidly to more than 30 countries and killing approximately 800 people (3). Both SARS-CoV and MERS-CoV infect airway and alveolar epithelial cells, resulting in acute respiratory illnesses (6). While there was 10% mortality among all SARS-CoV-infected patients, individuals aged 60 and above suffered worse outcomes, with a mortality rate of >50% (3). On a similar note, the newly emerging MERS-CoV infection is associated with an approximate mortality rate of 30% in humans (5). Although there has not been any known new incidence of SARS-CoV infection in humans, the recent emergence of MERS-CoV in humans and identification of SARS-like coronaviruses in bats and wild animals illustrate the potential threat of such pathogens.

Neutralizing (NT) antibody responses generated against spike (S) glycoprotein of SARS-CoV provide complete protection against SARS-CoV infection. Several potential vaccine candidates, such as attenuated virus vaccines, subunit constructs, and recombinant DNA plasmids, were shown to be protective in mouse models of SARS-CoV infection, largely by inducing a robust NT antibody response (7–11). Recent studies from our laboratory showed that attenuated mouse-adapted SARS-CoV (MA15) (12), which lacks the E protein (rMA15-ΔE), was safe and completely protective in susceptible 6-week-old and 12-month-old BALB/c mice. In addition to inducing NT antibody responses, rMA15-ΔE induced strong T cell responses (11, 13, 14). Cytotoxic T cells (CTL) play a crucial role in clearing respiratory viruses and can provide long-term protective cellular immunity (15, 16). SARS-CoV infection induces a potent and long-lived T cell response in surviving humans (17, 18). The majority of immunodominant T cell epitopes reside primarily in three structural proteins, the S, M, and N proteins, of SARS-CoV. Immunodominant CD8 T cell epitopes recognized in C57BL/6 (B6) mice include S525 and S436

**Received** 25 May 2014 **Accepted** 15 July 2014

**Published ahead of print** 23 July 2014

**Editor:** R. M. Sandri-Goldin

Address correspondence to Stanley Perlman, Stanley-perlman@uiowa.edu.



doi:10.1128/JVI.01505-14

(encompassing residues 525 to 532 and 436 to 443 of the spike protein) (19, 20).

Young (6- to 10-week-old) B6 mice are resistant to MA15 infection; however, as mice age, there is a steep increase in the susceptibility such that mice >6 months old are highly susceptible to the infection (21). As in many infections, virus-specific CD4 and CD8 T cells protect susceptible young and aged BALB/c and aged B6 mice following MA15 infection (19, 21, 22). The age-dependent susceptibility to MA15 is associated with a poor antiviral CD8 T cell response. We showed that increased PGD2 levels in the lungs of aged mice after MA15 infection was responsible, at least in part, for this poor T cell response by impairing migration of respiratory dendritic cells (rDCs) to draining lymph nodes (DLN). This led to reduced priming in the DLN and reduced MA15-specific CD8 T cell accumulation in the lungs compared to those in young mice (21). Although MA15-specific effector CD8 T cells are required for virus clearance during the acute infection, the role of memory CD8 T cells in protecting the host against subsequent lethal challenge is not known. Interestingly, SARS-CoV infection induced strong and long-lasting virus-specific T cells that were detectable for up to 6 years in patients who had recovered (17, 23). Since the memory B cell response and neutralizing antibodies are short-lived in SARS-CoV-infected patients, developing vaccines capable of generating long-lived memory CD8 T cells is desirable.

Antigen-specific memory CD8 T cells are categorized into three subpopulations. In addition to antigen-specific effector memory ($T_{EM}$) and central memory ($T_{CM}$) CD8 T cells, a population of tissue resident memory ($T_{RM}$) CD8 T cells exists in the peripheral tissues after a local pathogen encounter. $T_{RM}$ cells are nonmigratory and persist at the site of infection for a long period (24). These cells mediate rapid virus clearance from the site of infection upon pathogen challenge by secreting antiviral effector molecules, which limit virus replication (25), and expressing chemokines that recruit additional memory CD8 T cells from the circulation (26). An effective early T cell response to a respiratory virus challenge depends on the number of antigen-specific memory CD8 T cells in different lung compartments (27, 28). Further, the number and efficacy of virus-specific CD8 T cells in the lung airways correlate with the ability to clear a secondary virus challenge (29, 30).

In the current study, we examined whether a SARS-CoV-specific memory CD8 T cell response was sufficient to protect mice from lethal disease. Using a well-established prime-boost strategy to boost the number of memory CD8 T cells in the respiratory tract, we showed that SARS-CoV immunodominant epitope-specific memory CD8 T cells protected susceptible 8- to 10-month-old B6 mice from a lethal MA15 infection. Mice were primed intravenously with DCs loaded with peptide (S436 or S525) and then boosted intranasally with recombinant vaccinia virus (rVV) encoding S436 or S525. MA15-specific memory CD8 T cells generated in the lungs provided a significant level of protection from lethal MA15 challenge.

## MATERIALS AND METHODS

**Mice and viruses.** Pathogen-free female B6 mice (8 to 9 months old) were purchased from the National Cancer Institute (Frederick, MD). Mice were maintained in the University of Iowa animal care facility. All animal experiments were approved by the University of Iowa Institutional Animal Care and Use Committee (IACUC). MA15, a kind gift from Kanta Subbarao (NIH, Bethesda, MD), was propagated on Vero E6 cells (12).

Recombinant vaccinia viruses (rVVs) encoding S436 and S525 (referred to as rVV-S436 and rVV-S525) were engineered using the following complementary oligonucleotides: for S436, 5′-TCGACGCCACCATGTACAACTACAAGTACAGGTACCTGTAAGGTAC and 3′-CTTACAGGTACCTGTACTTGTAGTTGTACATGGTGGCG, and for S525, 5′-TCGACGCCACCATGGTGAACTTCAACTTCAACGGCCTGTAAGGTAC and 3′-CTTACAGGCCGTTGAAGTTGAAGTTCACCATGGTGGCG. The oligonucleotides were annealed and ligated into PSC65 (a VV shuttle vector with a strong synthetic VV early/late promoter, kindly provided by B. Moss, National Institutes of Health).

**Prime-boost immunization. (i) DC-peptide immunization.** Spleen-derived DCs were isolated from 6- to 8-week-old B6 mice previously inoculated subcutaneously with $1 \times 10^6$ B16 cells expressing Flt3L (provided by M. Prlic and M. Bevan, University of Washington). DCs were then harvested and pulsed as described previously (31). Briefly, $10^6$ lipopolysaccharide (LPS)-matured DCs (1 μg of LPS/mouse, intraperitoneally [i.p.] [*Salmonella enterica* serovar Abortusequi, S form, Enzo Lifesciences, Formingdale, NY]) were coated with 1 μM peptide (S436 or S525) for 2 h at 37°C. Peptide-pulsed DCs (referred to as DC-peptides) were then intravenously injected into 8- to 9-month-old B6 mice. Similar numbers of unpulsed DCs were injected into control mice. For detection of antigen-specific CD8 T cells, peripheral blood lymphocytes (PBL) were obtained by retro-orbital bleeding at different times postimmunization and analyzed for intracellular gamma interferon (IFN-γ) expression as described below.

**(ii) rVV minigenome booster.** At 6 days after DC-peptide immunization, mice were boosted by intranasal (i.n.) inoculation of rVV encoding either S436 or S525 ($2 \times 10^6$ PFU in 50 μl of Dulbecco modified Eagle medium [DMEM]). Mice were then rested for 42 to 45 days for memory studies.

**Challenge and survival studies.** To assess the protective ability of virus-specific memory CD8 T cells, prime-boost-immunized mice were challenged after 42 to 45 days by intranasal inoculation of $5 \times 10^4$ PFU of MA15 in 50 μl of DMEM. All infected mice were monitored daily for morbidity and mortality. Mice that lost 30% of their initial body weight were euthanized as per institutional IACUC guidelines. All challenge experiments were carried out in the animal biosafety level 3 (ABSL-3) laboratory as per approved guidelines.

**Virus titers in the lungs.** To obtain tissue for virus titer determination, mice were euthanized on different days postchallenge and lungs were homogenized in phosphate-buffered saline (PBS). Titers were determined on Vero E6 cells. Virus titers are represented as PFU/g of lung tissue.

**Preparation of cells from lungs, BAL, and spleen for fluorescence-activated cell sorting (FACS) analysis.** Mice were sacrificed at the time points indicated below and perfused via the right ventricle with 10 ml of PBS. Bronchoalveolar lavage fluid (BAL), lungs, and spleen were obtained. Lungs were cut into small pieces and digested in Hanks' balanced salt solution (HBSS) containing 2% fetal calf serum (FCS), 25 mM HEPES, 1 mg/ml of collagenase D (Roche), and 0.1 mg/ml of DNase (Roche) for 30 min at room temperature. Digested tissues were then minced and passed through a 70-μm nylon filter to obtain single-cell suspensions. Cells were enumerated by 0.2% trypan blue exclusion.

**Antibodies and flow cytometry.** The following monoclonal antibodies were used for these studies. Rat anti-mouse CD4 (RM4-5), rat anti-mouse CD8α (53-6.7), phycoerythrin (PE)-anti-IFN-γ (XMG1.2), allophycocyanin-anti-tumor necrosis factor alpha (APC-anti-TNF-α) (MP6-XT22), APC-anti-interleukin 2 (APC-anti-IL-2) (JES6-5H4), fluorescein isothiocyanate (FITC)-anti-CD107a/b, and PE-anti-CD69 (H1.2F3) were procured from BD Biosciences. PE-Cy7-anti-CD8 (53-6.7), rat anti-mouse IFN-γ (XMG1.2), hamster PE-anti-CD103 (2E7), V510-rat anti-mouse CXCR3 (CXCR3-173), and V450-anti-CD11a (M17/4) were purchased from eBioscience.

**Intracellular cytokine staining.** For intracellular cytokine staining, $1 \times 10^6$ cells per well were cultured in 96-well dishes at 37°C for 5 to 6 h in the presence of Golgiplug (1 μg) (BD Biosciences). The cells were blocked

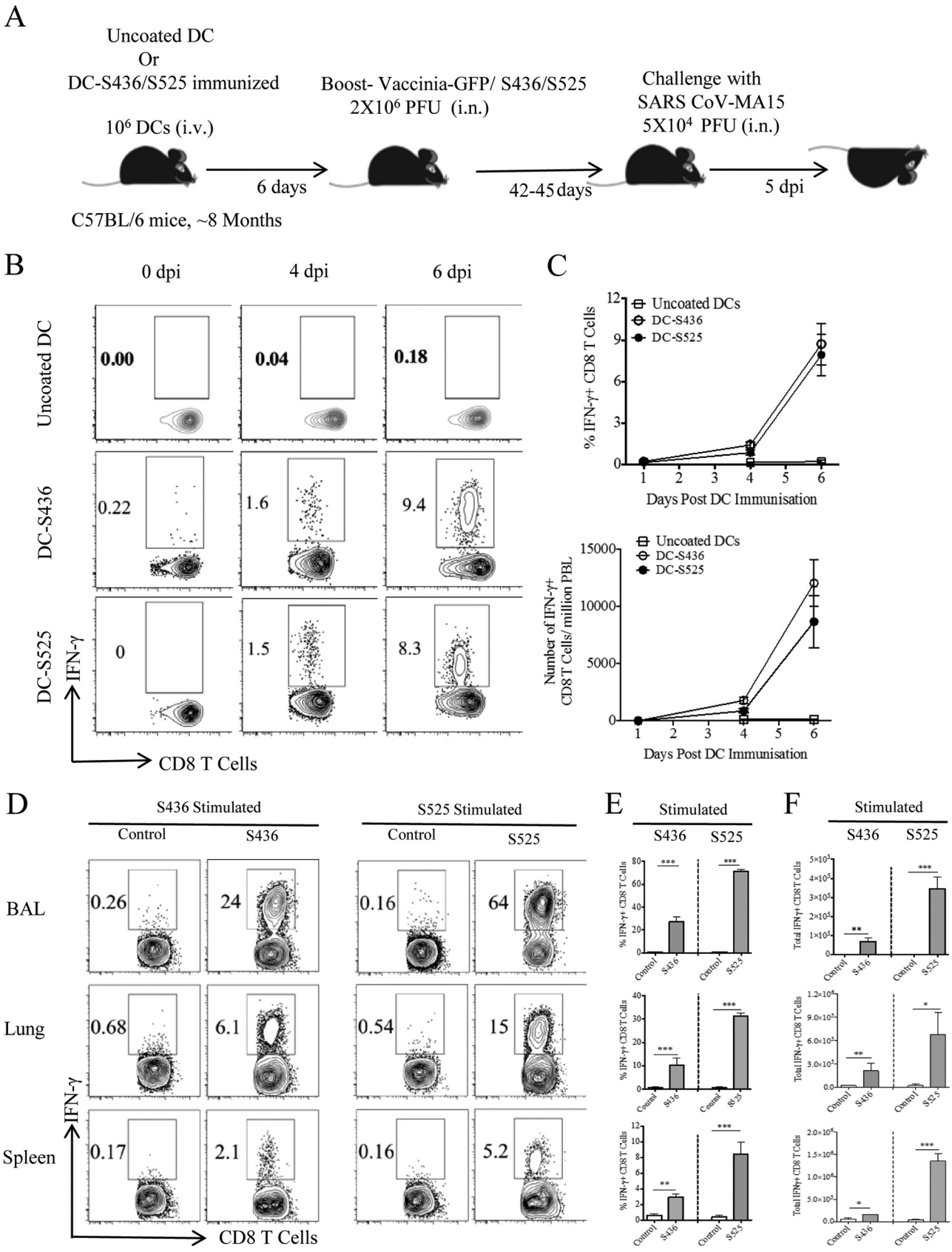
A
Uncoated DC
Or
DC-S436/S525 immunized
10⁶ DCs (i.v.)
6 days
Boost- Vaccinia-GFP/ S436/S525
2X10⁶ PFU (i.n.)
42-45 days
Challenge with
SARS CoV-MA15
5X10⁴ PFU (i.n.)
5 dpi
C57BL/6 mice, ~8 Months
B
0 dpi
4 dpi
6 dpi
Uncoated DC
DC-S436
DC-S525
0.00
0.04
0.18
0.22
1.6
9.4
0
1.5
8.3
IFN-γ
CD8 T Cells
C
Uncoated DCs
DC-S436
DC-S525
% IFN-γ+ CD8 T Cells
Days Post DC Immunisation
Number of IFN-γ+ CD8 T Cells/ million PBL
D
S436 Stimulated
S525 Stimulated
Control
S436
S525
BAL
Lung
Spleen
0.26
24
0.16
64
0.68
6.1
0.54
15
0.17
2.1
0.16
5.2
E
Stimulated
S436
S525
F
Stimulated
S436
S525
Total IFN-γ+ CD8 T Cells

with 1 μg of anti-CD16/32 antibody and surface stained with antibodies on ice. Cells were then fixed and permeabilized with Cytofix/Cytoperm solution (BD Biosciences) and labeled with anticytokine antibody. All flow cytometry data were acquired on a BD FACSVerse (BD Biosciences) and were analyzed using FlowJo software (Tree Star Inc.).

**Tetramer staining.** Major histocompatibility complex (MHC) class I/peptide tetramers, used to measure S436- and S525-specific CD8 T cells, was obtained from the NIH Tetramer Core Facility (Emory University, Atlanta, GA). A total of $5 \times 10^5$ to $1 \times 10^6$ cells obtained from BAL, lungs, and spleen of immunized or MA15-challenged mice were first incubated on ice with Fc block (anti-CD16/32 antibody) (BD Biosciences) for 15 min, followed by incubation with the APC-conjugated tetramer at 4°C for 30 min. Cells were then surface stained with PE-Cy7 anti-CD8 antibody. Flow cytometry data were acquired and processed as described above.

***In vivo* cytotoxicity assay.** *In vivo* cytotoxicity assays were performed on day 5 after infection, as previously described (32). Briefly, splenocytes from naive CD45.1 (Ly5.2) mice were labeled with either 1 μM or 100 nM carboxyfluorescein succinimidyl ester (CFSE; Molecular Probes). Labeled cells were then pulsed with peptides (5 μM) at 37°C for 1 h, and $5 \times 10^5$ cells from each group (peptide pulsed and nonpulsed) were mixed together. A total of $10^6$ cells were transferred intranasally (i.n.) into challenged mice, and total lung cells were isolated at 12 h after transfer. Target cells were distinguished from host cells on the basis of CD45.1 staining and from each other on the basis of CFSE staining. Percent specific lysis was determined as previously described (32).

**Lung histology.** Animals were anesthetized and transcardially perfused with PBS followed by zinc formalin. Lungs were removed, fixed in zinc formalin, and paraffin embedded. Sections were stained with hematoxylin and eosin and examined by light microscopy.

**Statistical analysis.** Data were analyzed using Student's *t* test. Results in the graphs below are represented as means ± standard errors of the means (SEM) unless otherwise mentioned. *P* values are represented in figures as follows: *, $P \leq 0.05$; **, $P \leq 0.01$; and ***, $P \leq 0.001$.

## RESULTS

**Prime-boost immunization induces a strong CD8 T cell response.** Recently, we and others identified and validated several CD8 T cell epitopes located in SARS-CoV structural proteins (19, 20). S436 and S525 were found to be immunodominant in B6 mice and were used in this study to evaluate virus-specific CD8 T cell responses. We adopted a prime-boost strategy to generate large numbers of virus-specific memory CD8 T cells in the BAL and lungs (31). Eight- to 9-month-old B6 mice were initially primed by intravenous injection of LPS-matured DCs loaded with S436 or S525 peptide (Fig. 1A). DC-peptide immunization resulted in a higher percentage and number of MA15-specific CD8 T cells in the peripheral blood (PBL) than in mice immunized with uncoated DCs. A kinetics study of DC-peptide immunization showed that a significant S436- and S525-specific CD8 T cell response was detected on day 4 after immunization and peaked at day 6 after DC-peptide immunization. The proportion and total number of epitope-specific CD8 T cells in PBL were similar in the DC-S436- and DC-S525-immunized groups (Fig. 1B and C). DC-peptide-primed mice were boosted 6 days later by intranasal inoculation of rVV-S436 or rVV-S525. Mice treated with uncoated DCs and boosted with rVV expressing green fluorescent protein (GFP) (rVV-GFP) were used as controls. Intranasal boosting with rVV-S436 or rVV-S525 generated a large pool of virus-specific effector CD8 T cells in the BAL, lungs, and spleen, with virus-specific cells detected at the highest frequency in the BAL (Fig. 1D and E). Additionally, the proportion and number of S525-specific CD8 T cells were significantly higher in BAL, lungs, and spleen than were those of S436-specific CD8 T cells ($P < 0.001$) (Fig. 1D to F). Collectively, these data indicate that prime-boost immunization resulted in the generation of large pools of S436- and S525-specific CD8 T cells in BAL and lungs.

**Induction of a MA15-specific memory CD8 T cell response after DC priming and rVV boosting.** An early protective response of virus-specific CD8 T cells to a respiratory virus challenge depends on the presence of an adequate number of antigen-specific memory CD8 T cells in the BAL and lungs (15). To determine the number of virus-specific memory CD8 T cells, mice were allowed to rest for 42 to 45 days after prime-boost immunization and the percentage and total number of S436- and S525-specific memory CD8 T cells were determined in the BAL, lungs, and spleen. The percentage and total number of S436- and S525-specific memory CD8 T cells were similar and were significantly higher in BAL, lungs, and spleen in the S436 and S525 prime-boost-immunized groups, respectively, than in mice immunized with rVV-GFP controls (Fig. 2A and B). Additionally, the proportion of virus-specific CD8 T cells among the total CD8 T cell pool was much higher for both the S436 and S525 groups in the lung airways (30 to 40%) than in the lungs (4 to 5%) or spleen (1 to 1.5%) (Fig. 2A). Since the protective ability of lung resident memory CD8 T cells to counter a local pathogen challenge depends upon their capacity to produce multiple antiviral effector molecules (33), we determined the polyfunctionality of the S436 and S525 memory CD8 T cells by assessing cytokine expression after *ex vivo* stimulation (33). As shown in Fig. 2C, a high percentage of total CD8 T cells isolated from the BAL secreted multiple cytokines, followed by those in the lungs and spleen, in both the S436 and S525 groups. The proportion of IFN-$\gamma^+$ CD8 T cells coexpressing TNF-α (double producers) and TNF-α and IL-2 (triple producers) was much higher in the BAL and lungs than in the spleen. In contrast, virus-specific CD8 T cells from spleen were mostly single-cytokine producers (IFN-$\gamma^+$ only) (Fig. 2C). Together, these results suggest that cells in the BAL and lungs are especially well positioned to respond effectively after challenge.

Virus-specific memory CD8 T cells in the lung airways, lung parenchyma, and secondary lymphoid organs are phenotypically distinct, with surface expression of markers such as CD103, CXCR3, and CD11a defining tissue resident versus nonresident memory CD8 T cells (16). To phenotypically distinguish virus-

**FIG 1** Prime-boost immunization induces a strong CD8 T cell response in 8-month-old mice. (A) Eight-month-old B6 mice were immunized intravenously (i.v.) with DC-loaded peptides and boosted 6 days later with rVV-S436 or rVV-S525 intranasally. Mice were rested for 42 to 45 days and then challenged with a lethal dose ($5 \times 10^4$ PFU) of MA15 (i.n.). Lungs and BAL were harvested 5 days postchallenge for further analysis. dpi, days postinfection. (B) FACS plots show percentages of S436- and S525-specific IFN-$\gamma^+$ CD8 T cells in the blood (after direct *ex vivo* stimulation with respective peptides) on 0, 4, and 6 days after DC-peptide immunization. (C) Mean percentages (top) and numbers (bottom) of S436- and S525-specific CD8 T cells in the blood are shown. (D) FACS plots represent percentages of S436- and S525-specific IFN-$\gamma^+$ CD8 T cells (after direct *ex vivo* stimulation with respective peptides) in BAL, lungs, and spleen 8 days after rVV-minigene boosting. (E and F) Bar graphs show mean percentages (E) and numbers (F) of S436- and S525-specific IFN-$\gamma^+$ CD8 T cells (after *in vitro* stimulation with respective peptides) in BAL, lungs, and spleen 8 days after rVV-minigene boosting. Data are representative of 2 independent experiments with 3 or 4 mice/group. *, $P < 0.05$; **, $P < 0.01$; ***, $P < 0.001$ (by unpaired two-tailed Student's *t* test).

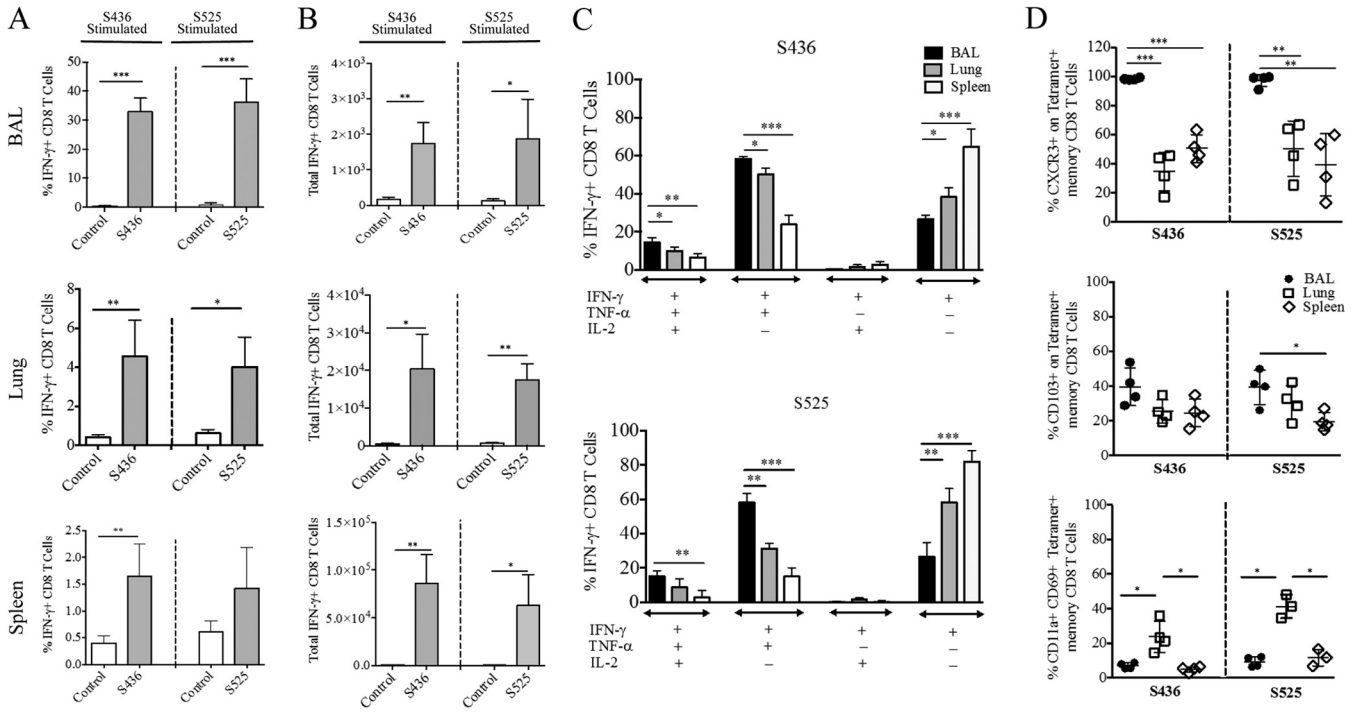


**FIG 2** Identification of SARS-CoV-specific memory CD8 T cells. Prime-boost-immunized mice were rested for 42 to 45 days, and the percentages and numbers of S436 and S525-specific memory CD8 T cells were determined in BAL, lungs, and spleen. (A and B) The bar graphs show mean percentages (A) and numbers (B) of S436- and S525-specific IFN-$\gamma^+$ CD8 T cells in the BAL, lungs, and spleen 42 to 45 days after rVV-minigene boosting. (C) The bar graphs show mean percentage of polyfunctional S436- and S525-specific IFN-$\gamma^+$ CD8 T cells in the BAL, lungs, and spleen. Data are means of cytokine-positive CD8 T cells obtained by Boolean gating. (D) Scatter plots represent the percentages of S436 and S525 CD8 T cells that express the indicated marker. Data are representative of 2 or 3 independent experiments with 3 or 4 mice/group. *, $P < 0.05$; **, $P < 0.01$; ***, $P < 0.001$ (by unpaired two-tailed Student's *t* test).

specific memory CD8 T cells in the lung airways, lung parenchyma, and spleen, we examined the expression of several molecules associated with tissue homing and activation. Expression of CXCR3, a molecule required for localization of memory T cells to lung airways, was significantly higher on S436- and S525-specific memory CD8 T cells from the lung airways (>95%) than on those isolated from the lung parenchyma (35 to 50%) and spleen (40 to 50%) (Fig. 2D). CD103, another marker of resident memory T cells, was also expressed on a high proportion of virus-specific CD8 T cells in the lung airway, followed by those in the lung parenchyma, with least CD103 expression on splenic CD8 T cells. CD11a and CD69, required for T cell activation and migration to tissues, are also upregulated on tissue resident memory T cells (34). As shown in Fig. 2D, a significantly higher proportion of S436- and S525-specific memory CD8 T cells in the lung parenchyma coexpressed CD11a and CD69 than in the lung airways and spleen, in agreement with previous studies (34).

**Analysis of virus-specific memory CD8 T cells following SARS-CoV challenge.** The ability of pathogen-specific memory CD8 T cells to protect the host from lethal challenge depends on their absolute number and on their ability to produce multiple effector cytokines (IFN-γ, TNF-α, and IL-2) and cytotoxic molecules (granzyme B and perforin) (35). To determine the magnitude and effector function of virus-specific CD8 T cells after pathogen exposure, prime-boost-immunized mice (now 10 to 11 months old) were challenged with a lethal dose ($5 \times 10^4$ PFU) of MA15 intranasally. Following MA15 challenge, the proportion and total number of S436- and S525-specific CD8 T cells were significantly higher in BAL and lungs of S436- and S525-immunized groups at day 5 postinfection (p.i.) than in the control group (Fig. 3A and B). Additionally, both the percentage and total number of virus-specific CD8 T cells were higher in the BAL and lungs of S525-immunized mice than for those immunized against the S436 epitope (74% versus 29% in BAL [$P < 0.001$] and 40% versus 24% in lungs [$P < 0.001$]; $3.5 \times 10^5$ versus $0.4 \times 10^5$ in BAL [$P < 0.001$] and $2.2 \times 10^6$ versus $0.4 \times 10^6$ in lungs [$P < 0.001$]) (Fig. 3A and B). To assess the functionality of the virus-specific CD8 T cells, we measured the ability of these cells to coproduce multiple effector cytokines. The majority of virus-specific CD8 T cells in both the S436- and S525-immunized groups coproduced IFN-γ and TNF-α but not IL-2 in the BAL and lungs (Fig. 3C). Since the BAL and lungs of control immunized mice had much lower percentages of virus-specific CD8 T cells (<1%) (Fig. 3A), we did not further analyze these cells.

To assess the cytotoxic ability of these virus-specific CD8 T cells, we measured granzyme B expression by S436- and S525-specific CD8 T cells in BAL and lungs following MA15 challenge. A significantly higher percentage of CD8 T cells from the BAL and lungs of the S436- and S525-immunized groups expressed granzyme B than from control mice (Fig. 4A and B). Further, CD8 T cells from S525-immunized mice expressed higher levels of granzyme B in both the BAL (48% versus 27%, $P < 0.01$) and lungs (53% versus 27%, $P < 0.001$) than did cells from S436-immunized mice. Moreover, CD8 T cells from the S436- and S525-immunized groups exhibited higher *in vivo* cytotoxic activity than did those from the control group. Notably, virus-specific CD8 T cells from the S525-

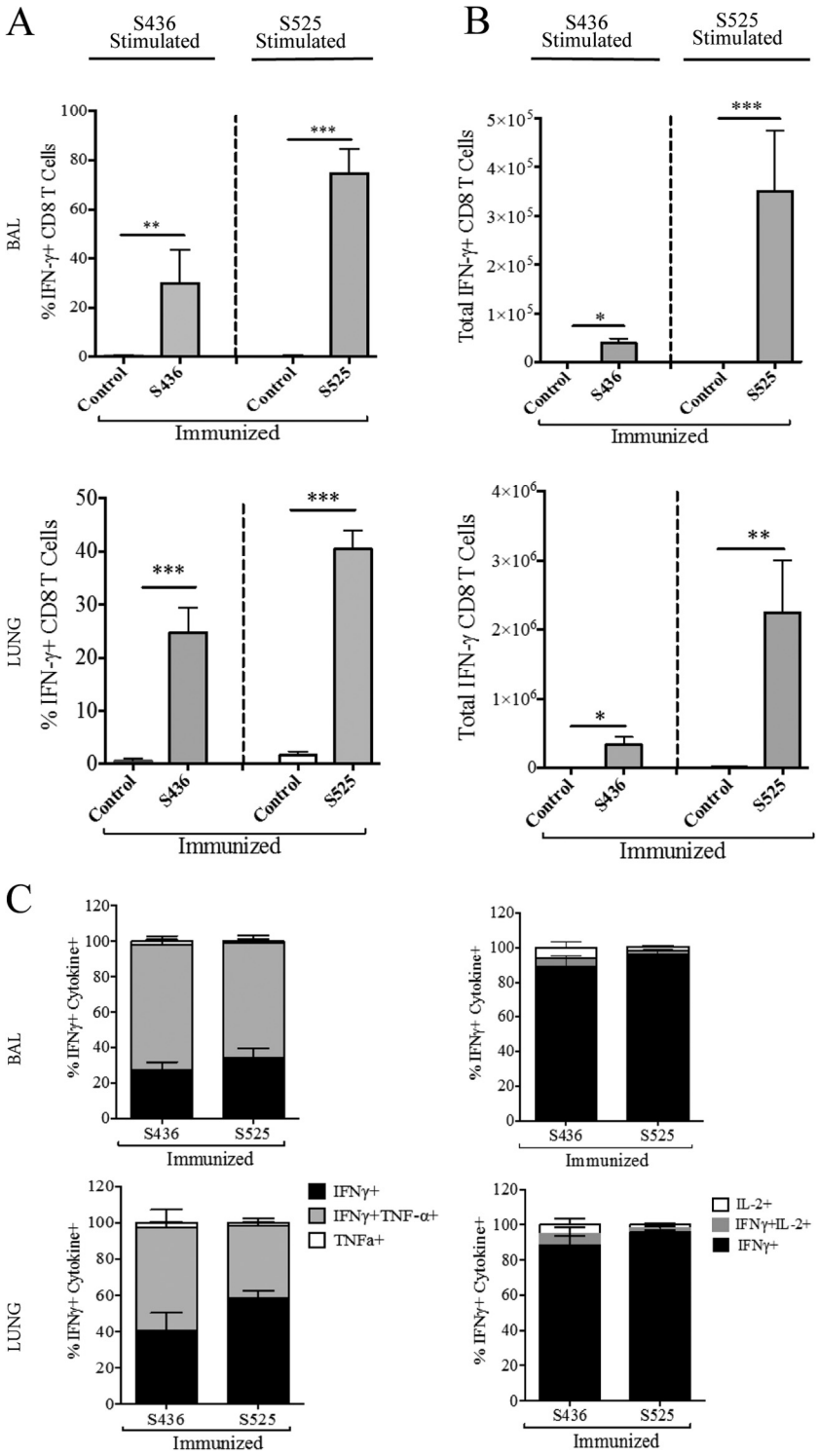


**FIG 3** Immunization induces polyfunctional secondary effector CD8 T cells. Prime-boost-immunized mice were rested for 42 to 45 days and then challenged with a lethal dose ($5 \times 10^4$ PFU) of MA15 (i.n.). Lungs and BAL were harvested 5 days postchallenge, and the percentage and number of epitope-specific CD8 T cells were determined. (A and B) The bar graphs show mean percentages (A) and numbers (B) of S436- and S525-specific IFN-$\gamma^+$ CD8 T cells (after direct *ex vivo* stimulation with respective peptides) in the BAL and lungs 5 days after MA15 challenge. (C) IFN-$\gamma^+$ CD8 T cells were further gated for TNF-α and IL-2 expression to determine polyfunctionality in the BAL and lungs. Data are representative of 3 independent experiments with 3 or 4 mice/group. *, $P < 0.05$; **, $P < 0.01$; ***, $P < 0.001$ (by unpaired two-tailed Student's *t* test).

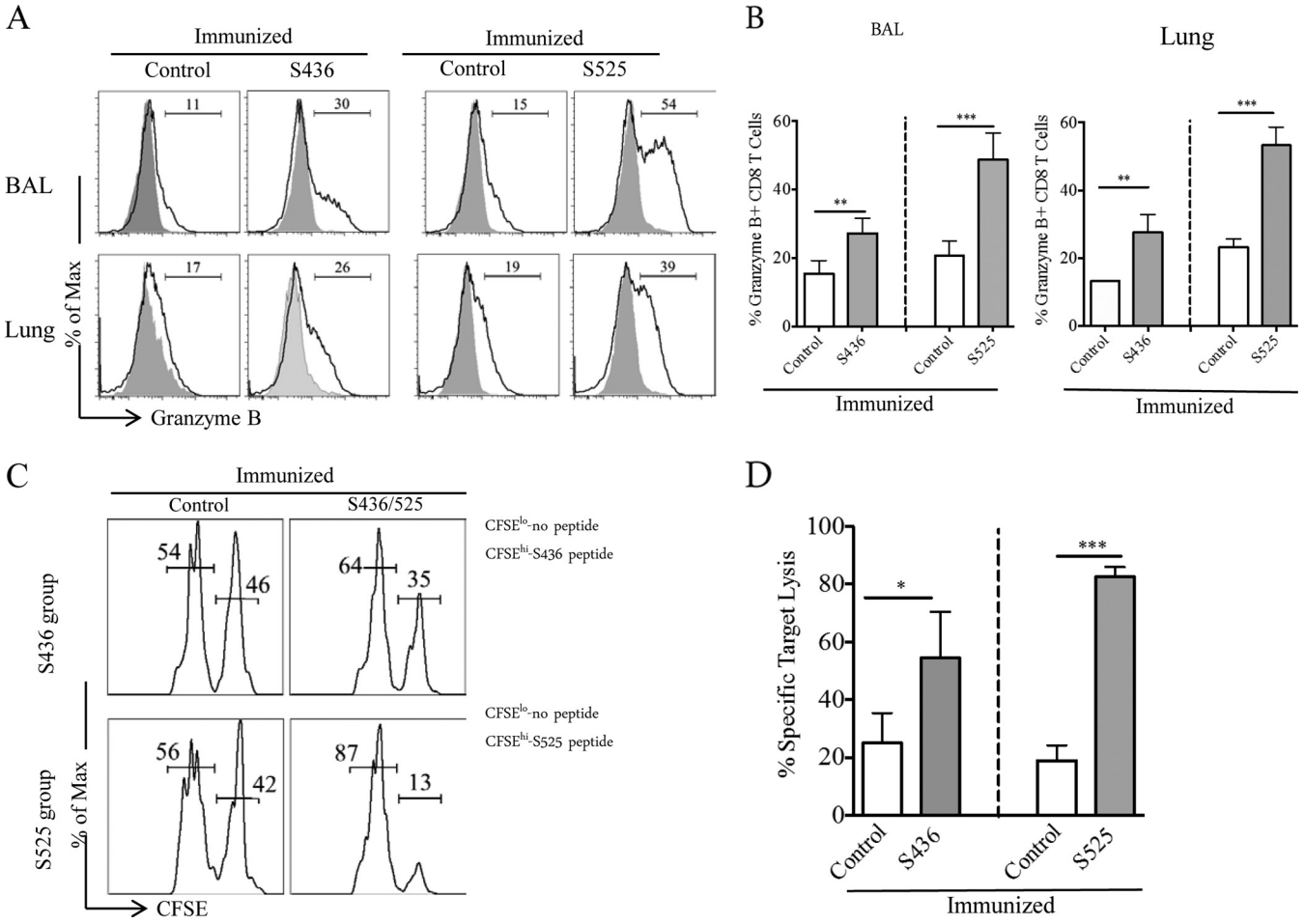


**FIG 4** Increased granzyme B production and cytotoxicity after challenge. (A and B) Histograms represent percent granzyme $B^+$ CD8 T cells in the BAL and lungs at day 5 after MA15 challenge (A). (B) Bar graphs represent mean percentage of granzyme $B^+$ CD8 T cells (after direct *ex vivo* stimulation with respective peptide). (C and D) *In vivo* cytotoxicity assays were performed 5 days after MA15 challenge, and the percent killing was calculated as described in Materials and Methods (numbers represent the percentage of cells labeled with different concentrations of CFSE). $n = 4$ or 5 mice/group/experiment. Data are representative of 2 independent experiments. *, $P < 0.05$; **, $P < 0.01$; ***, $P < 0.001$ (by unpaired two-tailed Student's *t* test).

immunized group were more cytotoxic than CD8 T cells from S436-immunized mice ($P < 0.005$) (Fig. 4C and D). This may reflect both enhanced intrinsic cytotoxicity and higher numbers of virus-specific CD8 T cells in the S525-immunized group (Fig. 3B and 4A and B). Thus, the prime-boost regimen generated tissue resident memory CD8 T cells that efficiently produced multiple effector cytokine and cytotoxic molecules upon MA15 challenge.

**Virus-specific memory CD8 T cells protect mice from lethal MA15 infection.** To investigate the protective effect of virus-specific memory CD8 T cells, prime-boost-immunized mice were challenged with a lethal dose of MA15 and monitored for morbidity and mortality. MA15-specific memory CD8 T cells protected immunized mice from lethal MA15 challenge to different extents. Consistent with the number of virus-specific memory CD8 T cells (Fig. 3A), immunization against epitope S525 protected approximately 80% of mice, while nearly 60% of mice survived in the S436-immunized group. Mice from both the S525- and S436-immunized groups lost approximately 20% of their initial body weight (Fig. 5A and B). In contrast, 100% of mice from the naive group and 80% of mice from the control-immunized group succumbed to the lethal infection (Fig. 5A and B). To determine whether protective efficacy could be further enhanced, we immunized an additional group of mice with a mixture of DC-525 and DC-436 and boosted them with rVV-525 and rVV-436. After challenge, approximately 85% of mice survived, only marginally different from the survival occurring after S525 immunization alone. No differences in weight were observed when the groups immunized with S525 and with S436 plus S525 were compared (Fig. 5A and B).

We next compared virus loads in lungs of immunized groups at different times after MA15 challenge. Immunization with S436 and S525 resulted in more rapid virus clearance than in control VV-GFP-immunized mice. Mice immunized with S436 or S525 had reduced viral burdens in the lungs as early as 4 days p.i. By 7 days postchallenge, 100% of S525-immunized mice and 50% of S436-immunized mice cleared the virus from lungs, while virus was not cleared in control mice (Fig. 5C). Histopathological examination of lungs of control mice on day 4 postinfection revealed marked alveolar edema, terminal bronchiolar epithelial sloughing, and thickening of interstitial septa, while that of S525-immunized mice revealed minimal amounts of alveolar edema but increased peribronchial lymphocytic infiltration (Fig. 5D). S436-

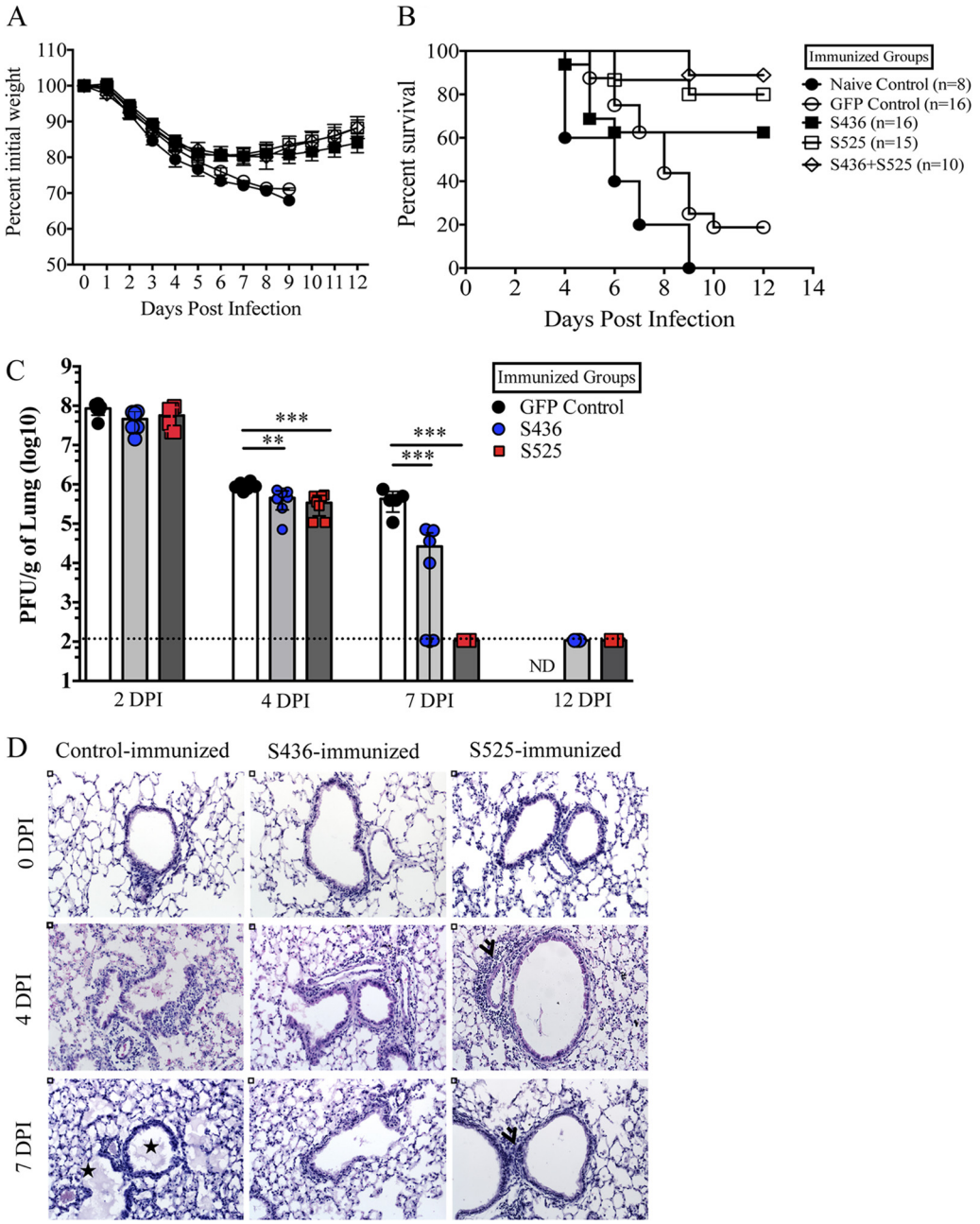


**FIG 5** Virus-specific memory CD8 T cells protect mid-aged mice from lethal MA15 infection. Prime-boost-immunized mice were rested for 42 to 45 days and then challenged with a lethal dose ($5 \times 10^4$ PFU) of MA15 intranasally. Percent initial body weight (A) and survival curves (B) are shown. The experiment shows data combined from three independent experiments, with 8 mice in the naive group and 15 or 16 mice in all other groups. Data are expressed as the percent initial weight ± the SEM. (C) Virus titers in lungs. Data correspond to means for 4 mice per group ± SEM and are representative of 2 or 3 independent experiments. (D) Lung sections from control and immunized mice are shown at days 0, 4, and 7 postchallenge. Stars represent alveolar and bronchiolar edema and arrowheads show peribronchial lymphocyte infiltration. DPI, days postinfection. *, $P < 0.05$; ** $P < 0.01$; ***, $P < 0.001$ (by unpaired Student's *t* test).

immunized mice showed histological features intermediate to control and S525-immunized mice. On day 7 p.i., lungs of control-immunized mice had marked alveolar and bronchiolar edema with thickened alveolar septa. At this time, pathological changes were reduced in both S436- and S525-immunized mice, especially in the latter group (Fig. 5D). Since immunization with S525 and with S436 plus S525 protected mice equivalently, no additional studies were performed on the dually immunized group. In summary, our results showed that memory CD8 T cells generated after prime-boost vaccination enhanced virus clearance, limited lung pathology, and protected susceptible B6 mice from lethal MA15 challenge.

## DISCUSSION

Only a limited number of studies have addressed the role of the T cell-mediated immune response in SARS-CoV infections. Previ-

ously, we demonstrated the ability of virus-specific CD8 T cells to protect susceptible young (BALB/c) and aged mice during a primary MA15 infection. In this study, we used a DC-rVV prime-boost regimen to generate a large number of virus-specific memory CD8 T cells in the BAL and lungs. SARS-CoV-specific memory CD8 T cells in the lungs exhibited a tissue resident memory phenotype and produced multiple effector cytokines and cytotoxic molecules. Our results show that SARS-CoV-specific memory CD8 T cells provided substantial protection against lethal MA15 challenge, with the extent of protection dependent on the specific immunodominant epitope used for immunization. Of note, DC-rVV prime-boost immunization did not induce SARS-CoV neutralizing antibodies measured 45 days after immunization, consistent with the notion that protection was mediated by memory CD8 T cells (data not shown). In this study, we analyzed 8- to 10-month-old infected mice because, like middle-aged humans, these mice were more susceptible to SARS-CoV than younger animals but more immunocompetent than very old mice. Following systemic primary immunization, effective CD8 T cell recall responses to a localized challenge depend upon antigen presentation by DCs in the DLN (36). Since DC migration to DLN is progressively impaired as mice age (21, 37), we adopted an intranasal boosting regimen to generate lung resident memory CD8 T cells, thereby minimizing the impact of DCs on the magnitude of the CD8 T cell recall response. The expansion of tissue resident memory CD8 T cells upon antigen rechallenge is largely independent of rDC migration to DLN, as local antigen presentation by epithelial cells, lung resident DCs, and recruited DCs drives memory CD8 T cell expansion (38). Intravenous priming with DC-peptide and intranasal boosting with rVV-minigene resulted in accumulation of SARS-CoV-specific memory CD8 T cells in BAL and lungs (Fig. 2).

Interestingly, we observed a change in immunodominance patterns of S436- and S525-specific CD8 T cells after rVV boosting and challenge. The proportion and total number of S436- and S525-specific CD8 T cells were similar at 6 days after DC-peptide immunization in the PBL and during the memory phase (42 to 45 days after rVV-minigene boosting) in all tissues (Fig. 1B and C and 2A and B). However, the proportion and the total number of S525-specific CD8 T cells were significantly higher than those of S436-specific CD8 T cells after rVV-minigene boosting (Fig. 1D to F) and after MA15 challenge (secondary effector response) (Fig. 3A and B). In mice infected with influenza A virus (IAV), CD8 T cell responses to the NP366 and PA224 epitopes are codominant, but upon rechallenge, the T cell response to epitope NP366 is dominant (39, 40). This change in epitope recognition was attributed to differences in antigen presentation (DCs versus nondendritic antigen-presenting cells [APCs]) (41). Such a mechanism might also explain differences in responses to S525 and S436, at least after MA15 challenge, although in this case, the two epitopes are located on the same viral protein.

We observed less protection against challenge in the S436-immunized than in S525-immunized mice, which is likely due to the lower number of S436-specific than of S525-specific CD8 T cells in the BAL and lungs (Fig. 3A and B) (35, 42, 43). Additionally, both S436- and S525-immunized mice cleared virus rapidly and exhibited reduced lung pathology compared to control mice. rVV boosting generated a substantial fraction of MA15-specific lung resident memory CD8 T cells, which provided protection upon subsequent challenge. These results are in agreement with recent studies demonstrating a critical role for lung resident virus-specific memory CD8 T cells in protecting the host from a lethal IAV challenge (44). Thus, intranasal immunization may be superior to systemic immunization because lung resident memory T cells are not generated if the immunogen is delivered systemically. Since systemic immunization does not result in the generation of lung resident memory CD8 T cells, protection is dependent upon constant replenishment from the periphery (27). Moreover, lung resident memory CD8 T cells generated after intranasal priming are required for optimal heterosubtypic IAV immunity. Lung resident memory CD8 T cells prevented extensive viral replication and limited alveolar damage, while circulating cells failed to protect against heterosubtypic challenge (44).

The protective ability of immunodominant epitope-specific CD8 T cells is of considerable significance, since SARS-CoV-specific antibody levels declined rapidly after recovery. SARS-CoV-specific IgM and IgA responses lasted less than 6 months, while IgG titers peaked at 4 months p.i. and markedly declined after 1 year (45–47). These studies suggested that the SARS-CoV-specific IgG antibody response would eventually disappear, and the peripheral memory B cell response would be insufficient for protection upon SARS-CoV reinfection. In contrast, SARS-CoV-specific memory CD8 T cells persisted for at least 6 years in patients who had recovered from SARS (45). Consequently, SARS-CoV-specific CD4 and CD8 T cells are likely to play a vital role in protecting patients upon SARS-CoV reinfection. Moreover, our results suggest that vaccine strategies aimed at achieving elevated numbers of tissue resident memory virus-specific CD8 T cells would be fruitful.

Of note, whether the T cell response is protective or pathogenic depends on the specific coronavirus and host strain (48). For example, following infection with MA15, MERS-CoV, or most strains of mouse hepatitis virus (MHV), virus-specific CD8 T cells are generally critical for virus clearance both during primary infection and secondary challenge (49, 50). In contrast, in C3H/HeJ mice infected with MHV-1, a pneumotropic strain of MHV, T cells moderately enhanced clinical illness and depletion of T cells ameliorated disease (51). Further, adoptive transfer of MHV-1-specific memory CD8 T cells in the absence of anti-MHV-1 antibody induced severe lung pathology and mortality in naive A/J and C3H/HeJ mice (51). In mice infected with the JHM strain of MHV, T cell-mediated virus clearance resulted in myelin destruction (52).

Although SARS has not recurred since its last pandemic in 2002-2003, the recent emergence of MERS-CoV in humans and porcine epidemic diarrhea virus in pigs highlights the need for coronavirus vaccines and antiviral agents. Our results indicate that in addition to a strong anti-SARS-CoV antibody response, an optimal memory CD8 T cell response will be an important goal in vaccine design.

## ACKNOWLEDGMENTS

We thank the NIH Tetramer Facility for providing MHC class I/peptide tetramers.

This work was supported in part by grants from the National Institutes of Health (AI091322 and AI060699).

## REFERENCES

1. **Fouchier RA, Kuiken T, Schutten M, van Amerongen G, van Doornum GJ, van den Hoogen BG, Peiris M, Lim W, Stohr K, Osterhaus AD.**

2003. Aetiology: Koch's postulates fulfilled for SARS virus. Nature **423:** 240. http://dx.doi.org/10.1038/423240a.

2. **Kuiken T, Fouchier RA, Schutten M, Rimmelzwaan GF, van Amerongen G, van Riel D, Laman JD, de Jong T, van Doornum G, Lim W, Ling AE, Chan PK, Tam JS, Zambon MC, Gopal R, Drosten C, van der Werf S, Escriou N, Manuguerra JC, Stohr K, Peiris JS, Osterhaus AD.** 2003. Newly discovered coronavirus as the primary cause of severe acute respiratory syndrome. Lancet **362:**263–270. http://dx.doi.org/10.1016/S0140-6736(03)13967-0.
3. **Peiris JS, Guan Y, Yuen KY.** 2004. Severe acute respiratory syndrome. Nat. Med. **10:**S88–S97. http://dx.doi.org/10.1038/nm1143.
4. **Zaki AM, van Boheemen S, Bestebroer TM, Osterhaus AD, Fouchier RA.** 2012. Isolation of a novel coronavirus from a man with pneumonia in Saudi Arabia. N. Engl. J. Med. **367:**1814–1820. http://dx.doi.org/10.1056/NEJMoa1211721.
5. **World Health Organization.** 2014. Middle East respiratory syndrome coronavirus (MERS-CoV)—update. World Health Organization, Geneva, Switzerland. http://www.who.int/csr/don/2014_03_25/en/.
6. **Graham RL, Donaldson EF, Baric RS.** 2013. A decade after SARS: strategies for controlling emerging coronaviruses. Nat. Rev. Microbiol. **11:** 836–848. http://dx.doi.org/10.1038/nrmicro3143.
7. **Gao W, Tamin A, Soloff A, D'Aiuto L, Nwanegbo E, Robbins PD, Bellini WJ, Barratt-Boyes S, Gambotto A.** 2003. Effects of a SARS-associated coronavirus vaccine in monkeys. Lancet **362:**1895–1896. http://dx.doi.org/10.1016/S0140-6736(03)14962-8.
8. **Yang ZY, Kong WP, Huang Y, Roberts A, Murphy BR, Subbarao K, Nabel GJ.** 2004. A DNA vaccine induces SARS coronavirus neutralization and protective immunity in mice. Nature **428:**561–564. http://dx.doi.org/10.1038/nature02463.
9. **Deming D, Sheahan T, Heise M, Yount B, Davis N, Sims A, Suthar M, Harkema J, Whitmore A, Pickles R, West A, Donaldson E, Curtis K, Johnston R, Baric R.** 2006. Vaccine efficacy in senescent mice challenged with recombinant SARS-CoV bearing epidemic and zoonotic spike variants. PLoS Med. **3:**e525. http://dx.doi.org/10.1371/journal.pmed.0030525.
10. **Graham RL, Becker MM, Eckerle LD, Bolles M, Denison MR, Baric RS.** 2012. A live, impaired-fidelity coronavirus vaccine protects in an aged, immunocompromised mouse model of lethal disease. Nat. Med. **18:** 1820–1826. http://dx.doi.org/10.1038/nm.2972.
11. **Enjuanes L, Dediego ML, Alvarez E, Deming D, Sheahan T, Baric R.** 2008. Vaccines to prevent severe acute respiratory syndrome coronavirus-induced disease. Virus Res. **133:**45–62. http://dx.doi.org/10.1016/j.virusres.2007.01.021.
12. **Roberts A, Deming D, Paddock CD, Cheng A, Yount B, Vogel L, Herman BD, Sheahan T, Heise M, Genrich GL, Zaki SR, Baric R, Subbarao K.** 2007. A mouse-adapted SARS-coronavirus causes disease and mortality in BALB/c mice. PLoS Pathog. **3:**e5. http://dx.doi.org/10.1371/journal.ppat.0030005.
13. **Fett C, DeDiego ML, Regla-Nava JA, Enjuanes L, Perlman S.** 2013. Complete protection against severe acute respiratory syndrome coronavirus-mediated lethal respiratory disease in aged mice by immunization with a mouse-adapted virus lacking E protein. J. Virol. **87:**6551–6559. http://dx.doi.org/10.1128/JVI.00087-13.
14. **DeDiego ML, Alvarez E, Almazan F, Rejas MT, Lamirande E, Roberts A, Shieh WJ, Zaki SR, Subbarao K, Enjuanes L.** 2007. A severe acute respiratory syndrome coronavirus that lacks the E gene is attenuated in vitro and in vivo. J. Virol. **81:**1701–1713. http://dx.doi.org/10.1128/JVI.01467-06.
15. **Kohlmeier JE, Woodland DL.** 2009. Immunity to respiratory viruses. Annu. Rev. Immunol. **27:**61–82. http://dx.doi.org/10.1146/annurev.immunol.021908.132625.
16. **Woodland DL, Scott I.** 2005. T cell memory in the lung airways. Proc. Am. Thorac. Soc. **2:**126–131. http://dx.doi.org/10.1513/pats.200501-003AW.
17. **Yang LT, Peng H, Zhu ZL, Li G, Huang ZT, Zhao ZX, Koup RA, Bailer RT, Wu CY.** 2006. Long-lived effector/central memory T-cell responses to severe acute respiratory syndrome coronavirus (SARS-CoV) S antigen in recovered SARS patients. Clin. Immunol. **120:**171–178. http://dx.doi.org/10.1016/j.clim.2006.05.002.
18. **Yang L, Peng H, Zhu Z, Li G, Huang Z, Zhao Z, Koup RA, Bailer RT, Wu C.** 2007. Persistent memory CD4+ and CD8+ T-cell responses in recovered severe acute respiratory syndrome (SARS) patients to SARS coronavirus M antigen. J. Gen. Virol. **88:**2740–2748. http://dx.doi.org/10.1099/vir.0.82839-0.
19. **Zhao J, Zhao J, Perlman S.** 2010. T cell responses are required for protection from clinical disease and for virus clearance in severe acute respiratory syndrome coronavirus-infected mice. J. Virol. **84:**9318–9325. http://dx.doi.org/10.1128/JVI.01049-10.
20. **Zhi Y, Kobinger GP, Jordan H, Suchma K, Weiss SR, Shen H, Schumer G, Gao G, Boyer JL, Crystal RG, Wilson JM.** 2005. Identification of murine CD8 T cell epitopes in codon-optimized SARS-associated coronavirus spike protein. Virology **335:**34–45. http://dx.doi.org/10.1016/j.virol.2005.01.050.
21. **Zhao J, Zhao J, Legge K, Perlman S.** 2011. Age-related increases in PGD(2) expression impair respiratory DC migration, resulting in diminished T cell responses upon respiratory virus infection in mice. J. Clin. Invest. **121:**4921–4930. http://dx.doi.org/10.1172/JCI59777.
22. **Chen J, Lau YF, Lamirande EW, Paddock CD, Bartlett JH, Zaki SR, Subbarao K.** 2010. Cellular immune responses to severe acute respiratory syndrome coronavirus (SARS-CoV) infection in senescent BALB/c mice: CD4+ T cells are important in control of SARS-CoV infection. J. Virol. **84:**1289–1301. http://dx.doi.org/10.1128/JVI.01281-09.
23. **Peng H, Yang LT, Wang LY, Li J, Huang J, Lu ZQ, Koup RA, Bailer RT, Wu CY.** 2006. Long-lived memory T lymphocyte responses against SARS coronavirus nucleocapsid protein in SARS-recovered patients. Virology **351:**466–475. http://dx.doi.org/10.1016/j.virol.2006.03.036.
24. **Slifka MK, Whitton JL.** 2000. Antigen-specific regulation of T cell-mediated cytokine production. Immunity **12:**451–457. http://dx.doi.org/10.1016/S1074-7613(00)80197-1.
25. **Kohlmeier JE, Cookenham T, Roberts AD, Miller SC, Woodland DL.** 2010. Type I interferons regulate cytolytic activity of memory CD8(+) T cells in the lung airways during respiratory virus challenge. Immunity **33:**96–105. http://dx.doi.org/10.1016/j.immuni.2010.06.016.
26. **Schenkel JM, Fraser KA, Vezys V, Masopust D.** 2013. Sensing and alarm function of resident memory CD8(+) T cells. Nat. Immunol. **14:**509–513. http://dx.doi.org/10.1038/ni.2568.
27. **Slütter B, Pewe LL, Kaech SM, Harty JT.** 2013. Lung airway-surveilling CXCR3(hi) memory CD8(+) T cells are critical for protection against influenza A virus. Immunity **39:**939–948. http://dx.doi.org/10.1016/j.immuni.2013.09.013.
28. **Wakim LM, Gupta N, Mintern JD, Villadangos JA.** 2013. Enhanced survival of lung tissue-resident memory CD8(+) T cells during infection with influenza virus due to selective expression of IFITM3. Nat. Immunol. **14:**238–245. http://dx.doi.org/10.1038/ni.2525.
29. **Hogan RJ, Usherwood EJ, Zhong W, Roberts AA, Dutton RW, Harmsen AG, Woodland DL.** 2001. Activated antigen-specific CD8+ T cells persist in the lungs following recovery from respiratory virus infections. J. Immunol. **166:**1813–1822. http://dx.doi.org/10.4049/jimmunol.166.3.1813.
30. **Ely KH, Cookenham T, Roberts AD, Woodland DL.** 2006. Memory T cell populations in the lung airways are maintained by continual recruitment. J. Immunol. **176:**537–543. http://dx.doi.org/10.4049/jimmunol.176.1.537.
31. **Pham NL, Badovinac VP, Harty JT.** 2009. A default pathway of memory CD8 T cell differentiation after dendritic cell immunization is deflected by encounter with inflammatory cytokines during antigen-driven proliferation. J. Immunol. **183:**2337–2348. http://dx.doi.org/10.4049/jimmunol.0901203.
32. **Barber DL, Wherry EJ, Ahmed R.** 2003. Cutting edge: rapid in vivo killing by memory CD8 T cells. J. Immunol. **171:**27–31. http://dx.doi.org/10.4049/jimmunol.171.1.27.
33. **Seder RA, Darrah PA, Roederer M.** 2008. T-cell quality in memory and protection: implications for vaccine design. Nat. Rev. Immunol. **8:**247–258. http://dx.doi.org/10.1038/nri2274.
34. **Teijaro JR, Turner D, Pham Q, Wherry EJ, Lefrancois L, Farber DL.** 2011. Cutting edge: tissue-retentive lung memory CD4 T cells mediate optimal protection to respiratory virus infection. J. Immunol. **187:**5510–5514. http://dx.doi.org/10.4049/jimmunol.1102243.
35. **Harty JT, Badovinac VP.** 2008. Shaping and reshaping CD8+ T-cell memory. Nat. Rev. Immunol. **8:**107–119. http://dx.doi.org/10.1038/nri2251.
36. **Zammit DJ, Cauley LS, Pham QM, Lefrancois L.** 2005. Dendritic cells maximize the memory CD8 T cell response to infection. Immunity **22:** 561–570. http://dx.doi.org/10.1016/j.immuni.2005.03.005.
37. **Grolleau-Julius A, Harning EK, Abernathy LM, Yung RL.** 2008. Impaired dendritic cell function in aging leads to defective antitumor immunity. Cancer Res. **68:**6341–6349. http://dx.doi.org/10.1158/0008-5472.CAN-07-5769.
38. **Wakim LM, Waithman J, van Rooijen N, Heath WR, Carbone FR.**

2008. Dendritic cell-induced memory T cell activation in nonlymphoid tissues. Science **319:**198–202. http://dx.doi.org/10.1126/science.1151869.
39. **Belz GT, Stevenson PG, Doherty PC.** 2000. Contemporary analysis of MHC-related immunodominance hierarchies in the CD8+ T cell response to influenza A viruses. J. Immunol. **165:**2404–2409. http://dx.doi.org/10.4049/jimmunol.165.5.2404.
40. **Belz GT, Xie W, Altman JD, Doherty PC.** 2000. A previously unrecognized H-2D(b)-restricted peptide prominent in the primary influenza A virus-specific CD8(+) T-cell response is much less apparent following secondary challenge. J. Virol. **74:**3486–3493. http://dx.doi.org/10.1128/JVI.74.8.3486-3493.2000.
41. **Crowe SR, Turner SJ, Miller SC, Roberts AD, Rappolo RA, Doherty PC, Ely KH, Woodland DL.** 2003. Differential antigen presentation regulates the changing patterns of CD8+ T cell immunodominance in primary and secondary influenza virus infections. J. Exp. Med. **198:**399–410. http://dx.doi.org/10.1084/jem.20022151.
42. **Christensen JP, Doherty PC, Branum KC, Riberdy JM.** 2000. Profound protection against respiratory challenge with a lethal H7N7 influenza A virus by increasing the magnitude of CD8(+) T-cell memory. J. Virol. **74:**11690–11696. http://dx.doi.org/10.1128/JVI.74.24.11690-11696.2000.
43. **Slütter B, Pewe LL, Lauer P, Harty JT.** 2013. Cutting edge: rapid boosting of cross-reactive memory CD8 T cells broadens the protective capacity of the Flumist vaccine. J. Immunol. **190:**3854–3858. http://dx.doi.org/10.4049/jimmunol.1202790.
44. **Wu T, Hu Y, Lee YT, Bouchard KR, Benechet A, Khanna K, Cauley LS.** 2014. Lung-resident memory CD8 T cells (TRM) are indispensable for optimal cross-protection against pulmonary virus infection. J. Leukoc. Biol. **95:**215–224. http://dx.doi.org/10.1189/jlb.0313180.
45. **Tang F, Quan Y, Xin ZT, Wrammert J, Ma MJ, Lv H, Wang TB, Yang H, Richardus JH, Liu W, Cao WC.** 2011. Lack of peripheral memory B cell responses in recovered patients with severe acute respiratory syndrome: a six-year follow-up study. J. Immunol. **186:**7264–7268. http://dx.doi.org/10.4049/jimmunol.0903490.
46. **Wu LP, Wang NC, Chang YH, Tian XY, Na DY, Zhang LY, Zheng L, Lan T, Wang LF, Liang GD.** 2007. Duration of antibody responses after severe acute respiratory syndrome. Emerg. Infect. Dis. **13:**1562–1564. http://dx.doi.org/10.3201/eid1310.070576.
47. **Woo PC, Lau SK, Wong BH, Chan KH, Chu CM, Tsoi HW, Huang Y, Peiris JS, Yuen KY.** 2004. Longitudinal profile of immunoglobulin G (IgG), IgM, and IgA antibodies against the severe acute respiratory syndrome (SARS) coronavirus nucleocapsid protein in patients with pneumonia due to the SARS coronavirus. Clin. Diagn. Lab. Immunol. **11:**665–668.
48. **Channappanavar R, Zhao J, Perlman S.** 21 May 2014. T cell-mediated immune response to respiratory coronaviruses. Immunol. Res. http://dx.doi.org/10.1007/s12026-014-8534-z.
49. **Williamson JS, Stohlman SA.** 1990. Effective clearance of mouse hepatitis virus from the central nervous system requires both CD4+ and CD8+ T cells. J. Virol. **64:**4589–4592.
50. **Zhao J, Li K, Wohlford-Lenane C, Agnihothram SS, Fett C, Zhao J, Gale MJ, Jr, Baric RS, Enjuanes L, Gallagher T, McCray PB, Jr, Perlman S.** 2014. Rapid generation of a mouse model for Middle East respiratory syndrome. Proc. Natl. Acad. Sci. U. S. A. **111:**4970–4975. http://dx.doi.org/10.1073/pnas.1323279111.
51. **Khanolkar A, Hartwig SM, Haag BA, Meyerholz DK, Epping LL, Haring JS, Varga SM, Harty JT.** 2009. Protective and pathologic roles of the immune response to mouse hepatitis virus type 1: implications for severe acute respiratory syndrome. J. Virol. **83:**9258–9272. http://dx.doi.org/10.1128/JVI.00355-09.
52. **Wu GF, Dandekar AA, Pewe L, Perlman S.** 2000. CD4 and CD8 T cells have redundant but not identical roles in virus-induced demyelination. J. Immunol. **165:**2278–2286. http://dx.doi.org/10.4049/jimmunol.165.4.2278.